Overview of electric machines for electric and hybrid vehicles

K.T. Chau* and Wenlong Li
Department of Electrical and Electronic Engineering, The University of Hong Kong, Pokfulam, Hong Kong
E-mail: ktchau@eee.hku.hk
* Corresponding author

Abstract: This invited paper gives an overview of various electric machines for application to electric vehicles (EVs) and hybrid electric vehicles (HEVs). First of all, the classification and a brief introduction of EVs and HEVs are presented. Then, viable electric machines that have been applied to EVs and HEVs, including the DC, induction, switched reluctance and permanent magnet (PM) brushless types, are reviewed. Consequently, the advanced PM machines that are promising for application to EVs and HEVs are discussed. Finally, the integrated PM machines are introduced, which are essential for future EVs and HEVs.

Keywords: electric machines; electric motors; electric vehicles; hybrid vehicles.

1 Introduction

In the past, there were various definitions of electric vehicles (EVs). They used to be classified into two types: the pure EV which was purely powered by batteries and only propelled by an electric motor, and the hybrid EV (HEV) which was powered by both batteries and liquid fuel while propelled by both the engine and the electric motor. After the invention of other energy sources, namely the fuel cells, ultracapacitors and ultrahigh-speed flywheels (Chau et al., 1999; Chau and Wong, 2001), this classification became inappropriate. In recent years, there has been a consensus that the EVs refer to vehicles with at least one of the propulsion devices being the electric motor. Then, when the energy source is only batteries and the propulsion device is only an electric motor, they are named as the battery EV (BEV) or loosely called the EV; when the energy source involves fuel cells working together with batteries and the propulsion device is only an electric motor, they are named as the fuel cell EV (FCEV) or simply called the fuel cell vehicle; when both batteries and liquid fuel are the energy sources while both the engine and the electric motor are the propulsion devices, they are named as the hybrid EV (HEV) or simply called the hybrid vehicle (Chan and Chau, 2001; Ehsani et al., 2005). Figure 1 depicts the classification of the internal combustion engine vehicle (ICEV), HEV, BEV and FCEV on the basis of the energy source and the propulsion device (Chau and Chan, 2007). Based on the hybridization level and the operation feature between the engine and the electric motor, the HEV has been further split into the micro hybrid (micro HEV), the mild hybrid (mild HEV) and the full hybrid (full HEV). Recently, this classification has been further extended to include the plug-in hybrid (PHEV) and the latest range-extended EV (REEV). They are also classified in terms of the energy source and the propulsion device as depicted in Figure 1.

The BEV, loosely termed the EV, offers the definite advantages of zero local emission (exhaust emission) and minimum global emission (taking into account the emission due to electricity generation by power plants). Its major drawbacks are the limited driving range, high initial cost and lack of fast charging infrastructure. In the next 5 years, the BEV will not be popular unless there is a breakthrough in battery technology in terms of specific energy, cycle life and cost per kilowatt-hour. The FCEV, loosely termed the fuel cell vehicle, offers the same advantages as the BEV – namely zero local emission and minimum global emission – while the driving range is comparable to that of an ICEV. Its major problems are the very high initial cost and lack of hydrogen refueling infrastructure. In the foreseeable future, the FCEV will not be commercially viable unless there is a breakthrough in fuel cell technology in terms of cost per kilowatt and operating conditions.

The HEV, loosely termed the hybrid vehicle, refers to the conventional or non-pluggable versions (Chau and Wong, 2002). For the micro hybrid, the conventional starter motor is eliminated while the conventional generator is replaced by a belt-driven integrated-starter-generator (ISG). Instead of propelling the vehicle, the ISG offers two important hybrid features. One feature is to shut down the engine whenever the vehicle is at rest, the so-called idle stop feature, hence improving the fuel economy for urban driving. Another feature is to recharge the battery primarily during vehicle deceleration or braking, thus offering a mild amount of regenerative braking. For the mild hybrid, the ISG is generally placed between the engine and the transmission. This ISG not only provides the hybrid features of idle stop and regenerative braking but also assists the engine to propel the vehicle, thus allowing for a downsized engine. However, since the engine and the ISG share the same shaft, it can not offer electric launch (initial acceleration under electric power only). For the full hybrid, the key technology is the electric variable transmission

(EVT) system which mainly functions to perform power splitting. This EVT can offer all hybrid features, including the electric launch, the idle stop, the regenerative braking and the engine downsizing.

The PHEV is extended from the conventional full hybrid by incorporating the additional feature of plug-in rechargeable. Since it incorporates a large bank of batteries which can be recharged by plugging to an external charging port, it can offer a long electric-drive range and hence reduce the requirement for refueling from gas stations. On the other hand, the REEV is extended from the BEV by incorporating a small engine coupled with a generator to recharge the battery bank. This avoids the range anxiety problem that is always associated with the BEV. So, it can offer energy-efficient operation throughout its electric-drive range and hence significantly reduce refueling from gas stations. Although the PHEV and the REEV are both a HEV and have similar electric motor and battery ratings, they have different nominal operations. The PHEV generally operates in the blended mode in which the electric motor and the engine are coordinated to work together in such a way that the engine can maintain efficient operation, hence achieving high fuel economy. In contrast, the REEV generally operates in the pure-electric mode all the way, regardless of the driving range or profile, until the battery pack is depleted to the threshold.

Electric machines are one of the core technologies for EVs. The general requirements of electric machines for EVs are much more stringent than those for industrial applications. These requirements are summarized below (Chan and Chau, 1997; Ehsani et al., 1997; Zhu and Howe, 2007):

- high torque density and high power density;
- wide speed range, covering low-speed creeping and high-speed cruising;
- high efficiency over wide torque and speed ranges;
- wide constant-power operating capability;
- high torque capability for electric launch and hill climbing;
- high intermittent overload capability for overtaking;
- high reliability and robustness for vehicular environment;
- low acoustic noise; and
- reasonable cost.

When the electric machine needs to work with the engine for various HEVs, there are some additional requirements:

- high-efficiency generation over a wide speed range;
- good voltage regulation over wide-speed generation; and
- capable of being integrated with the engine.

The purpose of this invited paper is to give an overview of electric machines for EVs and HEVs. Firstly, a review of electric machines that have been applied to EVs and HEVs, namely the DC, induction, switched reluctance (SR) and permanent magnet (PM) brushless types, will be conducted. Secondly, the classification of all electric machines that are viable for EVs and HEVs will be presented. Then, a review of those advanced PM machines will be conducted. Thirdly, the integrated PM machines will be brought forward for application to future EVs and HEVs.

It should be noted that this paper will focus on the discussion of topologies, operations, merits and demerits of those viable electric machines for EVs and HEVs. The corresponding power converters and control details will not be discussed. Also, this overview aims to provide a comprehensive introduction of all viable machine types, from a simple DC machine to a complex transverse-flux PM machine, rather than to give a critical assessment of particular machines. Readers who are in the field of vehicle design but new to the field of electric machines will benefit most from this overview.

2 Existing machines for EVs and HEVs

Among different types of electric machines, there are four types that have been adopted for EVs and HEVs, namely the DC, induction, SR, and PM brushless machines. They possess fundamentally different motor topologies as illustrated in Figure 2.

2.1 DC machines

DC machines used to be widely accepted for EVs. Based on the methods of field excitation, they can be grouped as the self-excited DC and separately excited DC types. Based on the source of field excitation, they can also be grouped as the wound-field DC and PM DC types (Dubey, 1989). As determined by the mutual interconnection between the field winding and the armature winding or the use of PM excitation, the whole family consists of the separately excited DC, shunt DC, series DC and PM DC types as shown in Figure 3. For the separately excited DC machine, the field and armature voltages can be controlled independent of each other. The torque-speed characteristic is linearly related that speed decreases as torque increases. For the shunt DC machine, the field and armature are connected to a common voltage source. The corresponding characteristic is similar to that of the separately excited DC machine. For the series DC machine, the field current is the same as the armature current. The torque-speed characteristic has an inverse relationship. For the PM

DC machine, the PM field is uncontrollable. Its torque-speed characteristic is similar to that of the shunt DC machine. It has relatively higher power density and higher efficiency because of the space-saving benefit by PMs and the absence of field losses.

All DC machines suffer from the same problem due to the use of commutators and brushes. Commutators cause torque ripples and limit the motor speed, while brushes are responsible for friction and radio-frequency interference. Moreover, due to the wear and tear, periodic maintenance of commutators and brushes is always required. These drawbacks make them less reliable and unsuitable for maintenance-free operation. The major advantages of DC machines are their maturity and simplicity. The simplicity is mainly due to their simple control because the air-gap flux Φ and the armature current I_a, hence the torque T, can be independently controlled as governed by:

$$T = K_e \Phi I_a \tag{1}$$

where K_e is named as the back electromotive force (EMF) constant or torque constant. However, because of their relatively low efficiency and need of maintenance, DC machines are no longer attractive for modern EVs or HEVs.

2.2 Induction machines

At present, induction machines are the most mature technology among various commutatorless machines. There are two types of induction machines, namely the wound-rotor and cage-rotor. Because of high cost, need of maintenance and lack of sturdiness, the wound-rotor induction machine is less attractive than the cage-rotor counterpart. Actually, the cage-rotor induction machine is loosely named as the induction machine. Apart from the common advantages of commutatorless machines such as the brushless and hence maintenance-free operation, the induction machine possesses the definite advantages of low cost and ruggedness.

Speed control of induction machines is considerably more complex than that of DC machines because of the nonlinearity of the dynamic model with coupling between direct and quadrature axes. Figure 4 shows two representative control operations, namely the variable-voltage variable-frequency (VVVF) control and the field-oriented control (FOC) which is also called vector control or decoupling control (Novotny and Lipo, 1996), that have been developed for electric propulsion.

The VVVF control strategy is based on constant volts/hertz control for frequencies below the rated frequency, whereas variable-frequency control with constant rated voltage for frequencies beyond the rated frequency. For very low frequencies, voltage boosting is applied to compensate the difference between applied voltage and induced EMF due to the stator resistance drop. Because of the disadvantages of air-gap flux drifting and sluggish response, the VVVF control is not suitable for high-performance EV operation such as the coordination of two in-wheel machines to implement electronic differential (Chan and Chau, 2001).

The FOC enables the induction machine being controlled alike the separately excited DC machine. By using coordinate transformation, the mathematical model of induction machines is transformed from the stationary reference frame (α-β frame) to the general synchronously rotating frame (x-y frame). When the x-axis is purposely selected to be coincident with the rotor flux linkage vector, the reference frame (d-q frame) becomes rotating synchronously with the rotor flux. Hence, the torque T can be expressed in terms of the d-axis stator current component i_{sd} and the q-axis stator current component i_{sq}:

$$T = \frac{3}{2} p \frac{M^2}{L_r} i_{sd} i_{sq} \quad (2)$$

where p is the number of pole pairs, M is the mutual inductance per phase and L_r is the rotor inductance per phase. This torque equation is very similar to that of the separately excited DC machine. Namely, i_{sd} resembles to Φ while i_{sq} resembles to I_a. Therefore, by means of this FOC, the torque can be effectively controlled to offer the desired fast transient response. With the advent of powerful low-cost microcontroller, the FOC-based induction machine has been widely adopted for modern EVs and HEVs.

2.3 SR machines

SR machines have been recognized to have considerable potential for EVs and HEVs (Rahman et al., 2000). They have the definite advantages of simple construction, low manufacturing cost and outstanding torque-speed characteristics (Miller, 1993). The operation principle of SR machines is based on the ‘minimum reluctance’ rule as shown in Figure 5. According to the co-energy principle, the reluctance torque T produced by one phase at any rotor position is given by:

$$T(\theta, i) = \frac{1}{2} i^2 \frac{dL}{d\theta} \quad (3)$$

where θ is the rotor position angle, i is the phase current and L is the phase inductance. There are two significant features. One is that the direction of torque is independent of the polarity of the phase current. Another is that the torque can be produced only in the direction of rising inductance ($dL/d\theta > 0$); otherwise, a negative torque (or braking torque) is produced. So, each phase can produce a positive torque only in half a rotor pole-pitch, hence creating the torque ripple. Also, because of the heavy saturation of pole tips and the fringing effect of poles and slots, they usually exhibit acoustic noise problems (Long et al. 2005).

The SR machines have basically two operation modes (Inderka et al., 2002). When the speed is below the base speed, the current can be limited by chopping, so-called current chopping control (CCC). In the CCC mode, the torque and thus the constant-torque characteristic can be controlled by changing the current limits. During high speed operation, however, the peak current is limited by the back EMF of the phase winding. The corresponding characteristic is essentially controlled by phasing of switching instants relative to the rotor position, so-called angular position control (APC). In the APC mode, the constant-power characteristic can be achieved.

In short, the SR machines have some fundamental problems hindering their application to EVs and HEVs – relatively low power density, control nonlinearity and acoustic noise. Over the years, their application to EVs and HEVs are limited.

2.4 PM brushless machines

PM brushless machines are becoming more and more attractive for EVs and HEVs (Chan et al., 1996). Their advantages are summarized below:

- Since the magnetic field is excited by high-energy PMs, the overall weight and volume can be significantly reduced for a given output power, leading to high power density.
- Because of the absence of rotor copper losses, their efficiency is inherently high.
- Since the heat mainly arises in the stator, it can be more efficiently dissipated to surroundings.
- Because of lower electromechanical time constant of the rotor, the rotor acceleration can be increased.

Nevertheless, the PM brushless machines suffer from the drawbacks of relatively high PM material cost and uncontrollable PM flux.

Based on the waveforms feeding into the machine terminals, the PM brushless machines can be divided into two main types (Pillay and

Krishnan, 1988) – the PM brushless AC (BLAC) and the PM brushless DC (BLDC). As shown in Figure 6, the PM BLAC machine is fed by sinusoidal or near-sinusoidal AC current, whereas the PM BLDC machine is fed by rectangular AC current. Actually, the PM BLAC machine is usually called the PM synchronous (PM Syn) machine (Chan and Chau, 1996). Since the interaction between trapezoidal field and rectangular current in the machine can produce higher torque product than that produced by sinusoidal field and sinusoidal current, the PM BLDC machine possesses higher power density than the PM Syn machine (Gan et al., 2000). Meanwhile, the PM BLDC has a significant torque pulsation (Kim et al., 1997), whereas the PM Syn produces an essentially constant instantaneous torque or so-called smooth torque like a wound-rotor synchronous machine.

According to the position of PMs in the rotor, PM brushless machines can be classified as the surface-mounted, surface-inset, interior-radial and interior-circumferential topologies as shown in Figure 7. For the surface-mounted topology, the PMs are simply mounted on the rotor surface by using epoxy adhesives. Since the permeability of PMs is near to that of air, the effective air-gap is the sum of the actual air-gap length and the radial thickness of the PMs. Hence, the corresponding armature reaction field is small and the stator winding inductance is low. Also, since the *d*-axis and *q*-axis stator winding inductances are nearly the same, its reluctance torque is almost zero. For the surface-inset topology, the PMs are inset or buried in the rotor surface. Thus, the *q*-axis inductance becomes higher than the *d*-axis inductance, hence producing an additional reluctance torque. Also, since the PMs are inside the rotor, it can withstand the centrifugal force at high-speed operation, hence offering good mechanical integrity. For the interior-radial topology, the PMs are radially magnetized and buried inside the rotor. Similar to the surface-inset one, the PMs are mechanically protected, hence allowing for high-speed operation. Also, because of its *d*-*q* saliency, an additional reluctance torque is generated. Different from the surface-inset one, this interior-radial topology adopts linear PMs which are easier for insertion and can be easily machinable. For the interior-circumferential topology, the PMs are circumferentially magnetized and buried inside the rotor. It takes the definite advantage that the air-gap flux density can be higher than the PM remanent flux density, the so-called flux focusing. Also, it holds the merits of good mechanical integrity and additional reluctance torque. However, because of significant flux leakage at the inner ends of PMs, a nonmagnetic shaft or collar is generally required. Each PM brushless machine topology can operate at both the BLAC and BLDC modes if the torque density, torque smoothness and efficiency are not of great concern.

For the PM Syn machine that operates with sinusoidal current and sinusoidal air-gap flux, the corresponding control operation is similar to that of the induction machine. So, based on the FOC, the torque T can be expressed as:

$$T = \frac{3}{2} p\left[\psi_m i_q - \left(L_q - L_d\right) i_d i_q\right] \qquad (4)$$

where p is the number of pole-pairs, ψ_m is the stator winding flux linkage due to the PMs, L_d , L_q are respectively the d-axis and q-axis stator winding inductances, and i_d , i_q are respectively the d-axis and q-axis currents. Moreover, the well-developed flux-weakening control technique that has been developed for the induction machine can readily be applied to the PM Syn machine for constant-power operation (Zhu et al., 2000; Soong and Ertugrul, 2002).

For the PM BLDC machine, the operation waveforms are no longer sinusoidal so that d-q axis transformation is ill-suited. Nevertheless, based on state equations, the torque T can be expressed as:

$$T = \frac{\left(e_a i_a + e_b i_b + e_c i_c\right)}{\omega_s} \qquad (5)$$

where e_a , e_b , e_c are the 3-phase back EMFs, i_a , i_b , i_c are the 3-phase armature currents, and ω_s is the synchronous speed. In the absence of d-q axis transformation, the constant-power operation of the PM BLDC machine is fundamentally different from that of the PM Syn machine. Specifically, its constant-power operation can be offered by using advanced conduction angle control (Safi et al., 1995; Chan et al., 1995) or by employing polygonal-winding interconnection (Wang et al., 2002).

2.5 Comparison of existing machines for EVs and HEVs

In order to evaluate the aforementioned machines for application to EVs and HEVs, they are compared in terms of their power density, efficiency, controllability, reliability, maturity, cost level, noise level and maintenance requirement. A point grading system (1 to 5 points) is used in which 1 is the worst and 5 is the best. As listed in Table 1, the key problem of the DC machine is the need of regular maintenance while the key drawback of the SR machine is the high acoustic noise, whereas the key merit of the induction machine is the low cost while the key advantages of PM brushless machines are the high power density and the high efficiency. This evaluation indicates that the commutatorless machines are preferred to the commutator one, namely the DC machine. Among those commutatorless machines, the induction machine and the PM brushless machines are most attractive. Between the two types of PM brushless machines, the PM BLDC machine can potentially offer better performance than the PM Syn machine.

Table 1 Evaluation of existing machines for EVs and HEVs

	DC	Induction	SR	PM Syn	PM BLDC
Power density	2	3	3.5	4.5	5
Efficiency	2	3	3.5	4.5	5
Controllability	5	4	3	4	4
Reliability	3	5	5	4	4
Maturity	5	5	4	5	4
Cost level	4	5	4	3	3
Noise level	3	5	2	5	5
Maintenance	1	5	5	5	5
Total	25	35	30	35	35

Table 2 Applications to flagship EVs and HEVs

Machine types	Car models
DC	Fiat Panda Elettra, Citroën Berlingo Electrique, Reva G-Wiz DC
SR	Chloride Lucas; Holden ECOmmodore
Induction	GM EV1, BMW Mini E, Tesla Roadster, Reva G-Wiz i; GM Chevy Volt, Imperia GP
PM Syn	Nissan Leaf, Mitsubishi i-MiEV, Citroën C-Zero, Peugeot iOn, BYD e6; Toyota Prius, Ford Fusion Hybrid
PM BLDC	Smart Fortwo ED; Honda Civic Hybrid

Table 2 summarizes the applications of various machines to flagship EVs and HEVs. For the DC machine, the applications are either obsolete or limited to those versions aspiring simplicity. For the SR machine, the applications are rare. Currently, the applications of the induction machine and the PM Syn machine almost equally share the market of both EVs and HEVs. With ever increasing concern on environmental protection and hence the demand of high energy efficiency, it is anticipated that the induction machine will be phasing out while the PM BLDC machine will be phasing in.

3 Advanced PM machines for EVs and HEVs

There are many topologies of electric machines, which create various classifications. Traditionally, they were classified into two groups – DC and AC. With the advent of new machine types, this classification becomes ill-suited. Figure 8 shows the proposed classification of electric machines in which the bold types are those that have been applied to EV and HEVs; meanwhile, the branches that are not viable for EVs and HEVs have been pruned. Basically, they are classified into two main groups – commutator and commutatorless. The former simply denotes that they have a commutator and carbon brushes, while the latter have neither commutator nor carbon brushes. It should be noted that the trend is focused on developing new types of PM commutatorless or brushless machines (Chau et al., 2008), especially the class of stator-PM machines and the class of variable reluctance (VR) PM machines.

3.1 Stator-PM machines

The stator-PM machine topologies are with PMs located in the stator, and generally with salient poles in both the stator and the rotor (Liu et al., 2008). Since the rotor has neither PMs nor windings, this class of machines is mechanically simple and robust, hence very suitable for vehicular operation. According to the location of the PMs, it can be split into the doubly-salient PM (DSPM), flux-reversal PM (FRPM) and flux-switching PM (FSPM) types. Additionally, with the inclusion of independent field or magnetizing windings in the stator for flux control, the class further derives the flux-controllable PM (FCPM) type. Their typical machine topologies are shown in Figure 9.

The DSPM machine is relatively the most mature type of stator-PM machines (Liao et al., 1995; Cheng et al., 2001; Cheng et al., 2003). Although it has salient poles in the stator and rotor, the PM torque significantly dominates the reluctance torque, hence exhibiting low cogging torque. Since the variation of flux linkage with each coil as the rotor rotates is unipolar, it is more suitable for the BLDC operation. The variation of air-gap flux of the DSPM machine is induced by the permeance variation, rather than by the PM rotation. Thus, by differentiating the co-energy, the torque T can be obtained as given by:

$$T = i\frac{d\Psi_{\mathrm{pm}}}{d\theta} + \frac{1}{2}i^2\frac{dL}{d\theta} = T_{\mathrm{pm}} + T_{\mathrm{r}} \tag{6}$$

where Ψ_{pm} is the PM flux linkage, L is the self inductance, i is the armature current, θ is the rotor position, T_{pm} is the PM torque component which is due to the interaction between armature current and PM flux linkage, and T_{r} is the reluctance torque component which is due to the variation of self inductance. The theoretical waveforms of Ψ_{pm} and L are shown in Figure 10. In order to make a unidirectional torque all the time, a bipolar armature current is used, in which a positive current is applied when the flux linkage increases whereas a negative current is applied when the flux linkage decreases. As a result, the PM torque becomes the dominant torque component, while the reluctance torque is a parasitic pulsating torque with a zero average value (Chau et al., 2005; Gong et al., 2009b). It should be noted that the operation of the DSPM machine is fundamentally different from that of the SR machine in which a unipolar armature current is adopted to create the reluctance torque only in the period of increasing inductance. Therefore, the torque density of this DSPM machine is inherently higher than that of the SR machine.

The FRPM machine exhibits the feature of bipolar flux linkage variation because the flux linkage with each coil reverses polarity as the rotor rotates (Deodhar et al., 1997). Each stator tooth has a pair of PMs of different polarities mounted onto each tooth surface. Since the bipolar flux linkage variation can have better utilization of iron core than the unipolar counterpart, the FRPM machine inherently offers higher torque density than the DSPM machine. However, since the PMs are attached on the surface of stator teeth, they are more prone to partial demagnetization. Also, significant eddy current loss in the PMs may be resulted.

The FSPM machine has attracted wide attention in recent years (Zhu et al., 2005). In this topology, each stator tooth consists of two adjacent laminated segments and a PM, and each of these segments is sandwiched by two circumferentially magnetized PMs. Hence, it enables flux focusing. Additionally, this flux-switching PM machine has less armature reaction, hence offering higher electric loading. Since its back EMF waveform is essentially sinusoidal, this machine is more suitable for the BLAC operation.

3.2 FCPM machines

In general, stator-PM machines suffer from the difficulty in air-gap flux control. Their constant-power operation ranges are limited, while some sophisticated operations such as on-line efficiency optimization or flux-strengthening operation cannot be achieved. One basic type of FCPM machines is the hybrid-field DSPM topology as shown in Figure 9 (Chau et al., 2003; Zhu et al., 2008). The stator incorporates two types of windings, namely the 3-phase armature winding and the DC field winding, and the PM poles. The rotor has neither PMs nor windings, hence offering high mechanical integrity. The 3-phase armature winding operates like that for the DSPM machine, whereas the DC field winding not only works as an electromagnet but also as a tool for flux control. Also, there is an extra air bridge in shunt with each PM. If the field winding magnetomotive force (MMF) reinforces the PM MMF, this extra flux path will assist the effect of flux strengthening. On the other hand, if the field winding MMF opposes the PM MMF, this extra flux path will favor the PM flux leakage, hence amplifying the effect of flux weakening. As a result, with a proper design of the air-bridge width, a wide flux-regulation range can be obtained by using a small DC field excitation. Its advantageous features are summarized below:

- By varying the polarity and magnitude of the DC field winding current, the air-gap flux density becomes easily controllable.
- By realizing flux strengthening, the machine can offer exceptionally high torque, which is very essential for electric launch for EVs or cold cranking for HEVs (Liu et al., 2010), or providing temporary power for overtaking and hill climbing. Typical torque waveforms with and without flux strengthening are depicted in Figure 11.
- By realizing flux weakening, the machine can offer the wide-speed constant-power feature, which is very essential for EV cruising.
- By online tuning the air-gap flux density, the machine can maintain constant-voltage output under generation or regeneration over a wide speed range, which is essential for battery charging for HEVs (Liu et al., 2010). Typical rectified output voltage waveforms with and without flux control are also depicted in Figure 11.
- By online tuning the air-gap flux density, the machine can offer efficiency-optimizing control (Liu et al., 2009a) or torque-ripple minimization (Zhu et al., 2009), which are highly desirable for EVs.

Although this topology takes the definite advantages of high mechanical integrity and flexible air-gap flux control which are highly desirable for EVs and HEVs, its stator is relatively bulky and the corresponding leakage flux is also significant. An improved version is to employ an outer-rotor topology (Chau et al., 2006). This outer-rotor topology can enable full utilization of the space of inner stator (the part beneath the armature winding) to accommodate both the PMs and the DC field winding, hence improving the power density. Also, since both the PMs and the DC field winding are embraced by the rotor, the problem of flux leakage can be minimized. However, this hybrid-field DSPM machine still suffers from a key drawback – the continual excitation of DC field winding for flux control will significantly increase the copper loss, hence deteriorating the inherent merit of high efficiency.

Recently, the concept of memory PM machines or flux-mnemonic PM machines has been proposed, which has the distinct ability to change the intensity of magnetization and also memorize the flux density level in the PMs (Ostovic, 2003). However, it suffers from complicated control of armature current for PM magnetization, and the possibility of accidental demagnetization due to armature reaction especially during regenerative braking. By incorporating the concept of memory PM machines into the outer-rotor hybrid-field DSPM machine, the memory DSPM machine is resulted, which can offer effective and efficient air-gap flux control (Yu et al., 2008). The high effectiveness is due to its direct magnetization of PMs by the magnetizing winding, while the high efficiency is due to the use of temporary current pulse for PM magnetization. The configuration of this machine is shown in Figure 12 which adopts a 5-phase outer-rotor double-layer-stator structure. The use of 5 phases rather than 3 phases is to enhance the torque smoothness which is desirable for vehicular operation. The use of double-layer-stator structure is to enable the PMs immune from accidental demagnetization by armature reaction.

Similar to the conventional memory PM machine, the PM material used in the memory DSPM machine is aluminum-nickel-cobalt (AlNiCo) alloy. Its demagnetization curve can offer a high remanent flux density B_r to enable high air-gap flux density, and a relatively low coercive force H_c to enable online demagnetization. Different from the conventional memory PM one, the PM magnetization of this machine is tuned by applying a current pulse to the magnetizing winding. Thus, it does not need to control the *d*-axis armature current, which is very complicated and may even conflict with the machine control strategy (Gong et al., 2009a). As depicted in Figure 12, the full magnetization is denoted by the operating point P_0 which is the intersection of the demagnetization curve and the load line. In order to lower the PM magnetization level, a negative current pulse is applied so that the operating point shifts from P_0 to Q_1. After this current pulse, it moves along the recoil line Q_1R_1 and then settles at P_1.

Similarly, in order to raise the PM magnetization level, a positive current pulse is applied so that the operating point shifts back to P_0. Therefore, by adjusting the magnitude and polarity of the current pulse, the PM magnetization level and hence the air-gap flux density can be flexibly controlled.

It should be noted that this memory DSPM machine can offer all operating features of the hybrid-field DSPM machine, namely the flux strengthening, flux weakening and flux optimization; meanwhile, the required energy consumption for PM magnetization or demagnetization is temporary and insignificant as compared with the energy consumption for continual hybrid-field excitation.

3.3 VR PM machines

The VR PM machine is a class of PM brushless machines dedicated to low-speed high-torque direct-drive applications. The operation principle is that the flux linkage to the armature winding changes along with the interaction between a set of PMs and a set of teeth. Generally, the pole-pair numbers excited by the stator armature winding and the rotor PMs are different. Based on the modulation function of the toothed-pole structure, the heteropolar fields can interact with one another to develop the steady torque (Harris, 1997). According to the relationship of motion plane and flux plane, the VR PM machines can be split into the vernier PM (VPM) machine and the transverse-flux PM (TFPM) machine types (Spooner and Haydock, 2003; Mueller and Baker, 2003).

The VPM machine is featured by its toothed-pole stator configuration. A small movement of the rotor can cause a large flux-linkage variation which makes a high torque. This is the so-called magnetic gearing effect. There are two typical topologies, namely the split-pole type and the open-slot type (Toba and Lipo, 1999). The former is suitable for high-resolution position control due to its large number of teeth. The latter has more space for housing coils, and is suitable for high-power application. Figure 13 shows the outer-rotor VPM machine topology which adopts the spilt-pole type (Li et al., 2010). It can be observed that each stator tooth is split into 3 small teeth at the end, which are called flux-modulation poles (FMPs). The inner-stator arrangement with FMPs enables to adopt the compact armature winding. Also, the armature winding adopts the coil pitch equal to the slot pitch, which can minimize the end-winding, hence saving the copper material and reducing the copper loss. The PMs are radially-magnetized and then surface-mounted on the rotor. Thanks to these FMPs, the fields excited by the stator armature winding and the rotor PMs with different pole-pair numbers can interact with each other. The outer-rotor arrangement inherently provides a large diameter to accommodate a large number of PM poles, hence enabling full utilization of the stator inner space to accommodate the armature winding. In addition, this low-speed high-torque outer rotor is particularly attractive for in-wheel direct-drive for EVs, thus eliminating the mechanical gear and improving the mechanical integrity.

There exists a fundamental rule governing the design of this VPM machine:

$$P_r = N_s \pm P_s \tag{7}$$

where P_r is the number of PM pole-pairs in the rotor, N_s is the number of FMPs in the stator and P_s is the number of armature winding pole-pairs in the stator. Based on the magnetic gearing effect, the output mechanical speed at the rotor is scaled down by multiplying a factor of P_s / P_r to the rotating field speed at the stator. For instance, when the stator is occupied by the 3-phase armature winding with 6 poles ($P_s = 3$) and there are 48 PM poles on the rotor ($P_r = 24$), the output speed is reduced by 8 times.

The TFPM machine is featured by its assembled stator and sandwiched PM rotor. It is renowned for its high torque density for direct-drive applications, especially for in-wheel drives (Baserrah et al., 2009). Based on the orientation of PMs, the TFPM machine can be split into the surface-magnet and flux-concentrated types. Namely, the PMs in the former type are magnetized in the axial direction and perpendicular to the direction of rotation, whereas PMs in the latter type are magnetized in the tangential direction and parallel to the direction of rotation. Since the flux-concentrated type can offer higher torque density than the surface-magnet type, it is particularly attractive for in-wheel drives though it is mechanically difficult in construction. On the other hand, the TFPM machine can be assembled by using U-shaped stator cores (Weh et al., 1988) or C-shaped stator cores (Li and Chau, 2010). The U-shaped type involves too many components which make the structure complicated and cause manufacturing difficulty, whereas the C-shaped type takes the definite advantage of simple structure and can provide a larger cross-sectional area for the armature winding, leading to further increase the electric loading and hence the torque density. Figure 13 shows the TFPM machine topology which adopts the C-shaped stator cores.

Since the magnetic flux paths via the stator cores are always orthogonal to the current flow in the armature winding, the magnetic loading is totally decoupled from the electric loading. Hence, the torque density of this TFPM machine outperforms that of other PM brushless machines. However, because of its flux path inherently three-dimensional, the corresponding design and structure are complicated, leading to fabrication difficulty and high manufacturing cost. Also, the corresponding electromagnetic analysis inevitably involves tedious numerical computation (Wang et al., 2008). Moreover, due to its severe flux leakage, the TFPM machine usually suffers from very low power factor.

3.4 Comparison of advanced PM machines for EVs and HEVs

Since the aforementioned advanced PM machines are still at the developing stage for application to EVs and HEVs, their performances have not been fully unveiled. Nevertheless, a qualitative comparison among them is given in Table 3, aiming to give an indicative assessment on their suitability for EVs and HEVs.

In terms of their power density and torque density, the TFPM machine is the best because of its inherent compact design. The VPM machine also outperforms the others in torque density because it inherently offers the low-speed operation. In terms of their efficiency, the FCPM machine is relatively the best due to its capability of flux control for efficiency optimization, whereas the VPM and TFPM machines suffer from high copper loss due to their low power factor. The FCPM machine, including both the hybrid-field and memory PM types, offers the definite advantage of superb flux controllability. Concerning the immunity of PMs from accidental demagnetization, the FRPM machine is relatively weak since the PMs mounted on the surface of stator teeth are more vulnerable to partial irreversible demagnetization. In contrast, the FSPM machine locates the PMs in such a way that the influence of armature reaction field on their working point is minimal, hence offering good PM immunity. In terms of mechanical robustness, the DSPM machine is relatively the best because of its simple magnetic structures, whereas the TFPM machine suffers from the complicated structure of three-dimensional flux path. The manufacturability is mainly based on the structural complexity, with an additional consideration of the control complexity. Thus, the DSPM machine can enjoy the merit of easy to manufacture, whereas the FCPM and TFPM machines suffer from the shortcoming of hard to manufacture. Finally, in terms of their maturity, the DSPM machine is relatively most mature, while the FCPM and VPM machines are less developed.

All these advanced PM machines have their own merits and demerits. The importance of their merits and demerits also varies with the types of application for EVs and HEVs. For instance, the DSPM machine is readily applied to the latest EVs and HEVs because it has been well developed and is relatively the most mature one. The FSPM machine is attractive for near-term application to EVs and HEVs because of its all-round performances. Meanwhile, the FCPM machine is attractive for those high-performance EVs which desire a wide constant-power operating range, and preferable for those high-performance HEVs where the ISG needs to provide a high starting torque for engine cranking and a constant generated voltage over a wide speed range. For in-wheel direct-drive EVs, the VPM machine is particularly attractive because of its low-speed nature with high torque density.

Table 3 Evaluation of advanced PM machines for EVs and HEVs

	DSPM	FRPM	FSPM	FCPM	VPM	TFPM
Power density	Medium	Good	Good	Good	Good	Superb
Torque density	Medium	Good	Good	Good	Superb	Superb
Efficiency	Good	Good	Good	Superb	Medium	Medium
Controllability	Medium	Medium	Good	Superb	Good	Good
PM immunity	Medium	Weak	Good	Medium	Medium	Medium
Robustness	Strong	Medium	Medium	Medium	Medium	Weak
Manufacturability	Easy	Medium	Medium	Hard	Medium	Hard
Maturity	High	Medium	Medium	Low	Low	Medium

4 Integrated PM machines for EVs and HEVs

The development of electric machines is no longer limited to design and operation of a particular machine. Actually, the latest research direction has been extended to system integration. In the following, two emerging integrated PM machine technologies are discussed, namely the integration of magnetic gear and PM brushless machine for EVs, and the integration of PM brushless machines and EVT for HEVs.

4.1 Integrated magnetic-geared PM brushless machines

For EVs, PM brushless machines are attractive since they inherently offer high power density and high efficiency. In addition, the use of PM brushless machines as the in-wheel machines can play the role of electronic differential (Chan and Chau, 2001). As the wheel speed is only about 600 rpm, the in-wheel PM brushless machine is either a low-speed gearless outer-rotor one or a high-speed planetary-geared inner-rotor one. Although the outer-rotor one takes the advantage of gearless operation, its low-speed operation causes bulky size and heavy weight. On the other hand, although the inner-rotor one takes the merits of reduced overall size and weight, the planetary gear inevitably involves transmission loss, acoustic noise and regular lubrication.

Recently, magnetic gears are becoming attractive, since they inherently offer the merits of high efficiency, reduced acoustic noise, and maintenance free (Atallah and Howe, 2001; Jian et al., 2009). They can adopt the interior-magnet arrangement (Liu et al., 2009b) or Halbach-magnet array (Jian and Chau, 2010a) to further improve their performances. By artfully integrating the magnetic gear into a PM BLDC machine, the integrated magnetic-geared PM BLDC machine is resulted in which the low-speed requirement for direct-drive and the high-speed requirement for machine design can be achieved simultaneously (Chau et al., 2007). Figure 14 gives a schematic comparison of the existing planetary-gear inner-rotor topology and the integrated magnetic-geared outer-rotor topology for in-wheel drives. It can be seen that the outer-rotor topology not only offers reduced size and weight, but also eliminates all the drawbacks due to the mechanical gear. Its detailed structure is shown in Figure 15. The artfulness is the share of a common PM rotor, namely the outer rotor of a PM BLDC machine and the inner rotor of a concentrically arranged magnetic gear.

The operation principle of this integrated magnetic-geared PM BLDC machine is similar to that of a high-speed planetary-geared inner-rotor machine, but with the difference that this one is an outer-rotor machine. Namely, the motoring operation is the same as the PM BLDC machine. For instance, the stator is fed by 3-phase rectangular currents, which are rated at 220 Hz, to achieve the rated speed of 4400 rpm. Then, the magnetic gear steps down the rated speed to 600 rpm, which in turn boosts up the torque by about 7 times for direct driving as also depicted in Figure 15.

4.2 Integrated EVT PM brushless machines

For HEVs, the EVT system mainly functions to perform power splitting of the internal combustion engine (ICE) output – one power flow path is to mechanically couple the ICE output with the motor output; while another power flow path is to electrical connect the generator output with the motor input via two power converters (Miller, 2006). Hence, a continuously variable ratio between the ICE speed and the wheel speed can be achieved. In the presence of this electronic continuously variable ratio, the ICE can always operate at its most energy-efficient operation point, resulting in a considerable reduction of fuel consumption.

Figure 16 gives a comparison of the existing planetary-geared EVT

PM brushless machine system which was developed by Toyota for its Prius (Kamiya, 2006) and the integrated magnetic-geared EVT PM brushless machine system (Jian and Chau, 2010b). The former one inherits the fundamental drawback of planetary gearing, namely the transmission loss, gear noise and need of regular lubrication. On the contrary, the latter one inherits the distinct advantages of magnetic gearing, namely the noncontact torque transmission and speed variation using the modulation effect of PM fields, hence achieving high transmission efficiency, silent operation and maintenance free. Also, the corresponding mechanical torque transmission is straightforward, simply from the ICE at one side to the driveline at another side, without requiring any transmission belts.

5 Conclusion

In this invited paper, a comprehensive overview of electric machines for EVs and HEVs has been presented, with emphasis on the machine topologies, operations, merits and demerits. Particularly, the existing machines that have been applied to EVs and HEVs are critically compared, confirming that the PM brushless machines continually play the major role. Increasingly, the advanced PM machines that are viable for EVs and HEVs are discussed, indicating that the class of stator-PM machines is highly attractive. Finally, the integrated PM machines that have high potential for future EVs and HEVs are introduced, deducing that the incorporation of magnetic gear into the PM brushless machine is promising.

Acknowledgment

This work was supported by a grant (Project No. HKU710710E) from the Hong Kong Research Grants Council, Hong Kong Special Administrative Region, China.

References

Atallah, K. and Howe, D. (2001) ‘A novel high performance magnetic gear,’ *IEEE Transactions on Magnetics*, Vol. 37, No. 4, July, pp. 2844-2846.

Baserrah, S., Rixen, K. and Orlil, B. (2009) ‘Transverse flux machines with distributed windings for in-wheel applications’, *Proc. IEEE Int. Conf. on Power Electronics and Drive Systems*, Taipei, November, pp. 102-108.

Chan, C.C. and Chau, K.T. (1996) ‘An advanced permanent magnet motor drive system for battery-powered electric vehicles', *IEEE Transactions on Vehicular Technology*, Vol. 45, No. 1, February, pp. 180-188.

Chan, C.C. and Chau, K.T. (1997) 'An overview of power electronics in electric vehicles', *IEEE Transactions on Industrial Electronics*, Vol. 44, No. 1, February, pp. 3-13.

Chan, C.C. and Chau, K.T. (2001). *Modern Electric Vehicle Technology*. Oxford University Press.

Chan, C.C., Chau, K.T., Jiang, J.Z., Xia, W., Zhu, M. and Zhang, R. (1996) 'Novel permanent magnet motor drives for electric vehicles', *IEEE Transactions on Industrial Electronics*, Vol. 43, No. 2, April, pp. 331-339.

Chan, C.C., Jiang, J.Z., Xia, W. and Chau, K.T. (1995) 'Novel wide range speed control of permanent magnet brushless motor drives', *IEEE Transactions on Power Electronics*, Vol. 10, No. 5, September, pp. 539-546.

Chau, K.T. and Chan, C.C. (2007) 'Emerging energy-efficient technologies for hybrid electric vehicles', *IEEE Proceedings*, Vol. 95, No. 4, April, pp. 821-835.

Chau, K.T. and Wong, Y.S. (2001) 'Hybridization of energy sources in electric vehicles', *Energy Conversion and Management*, Vol. 42, No. 9, June, pp. 1059-1069.

Chau, K.T. and Wong, Y.S. (2002) 'Overview of power management in hybrid electric vehicles', *Energy Conversion and Management*, Vol. 43, No. 15, June, pp. 1953-1968.

Chau, K.T., Chan, C.C. and Liu, C. (2008) 'Overview of permanent-magnet brushless drives for electric and hybrid electric vehicles', *IEEE Transactions on Industrial Electronics*, Vol. 55, No. 6, June, pp. 2246-2257.

Chau, K.T., Jiang, J.Z. and Wang, Y. (2003) 'A novel stator doubly fed doubly salient permanent magnet brushless machine', *IEEE Transactions on Magnetics*, Vol. 39, No. 5, September, pp. 3001-3003.

Chau, K.T., Li, Y.B., Jiang, J.Z. and Liu, C. (2006) 'Design and analysis of a stator doubly fed doubly salient permanent magnet machine for automotive engines', *IEEE Transactions on Magnetics*, Vol. 42, No. 10, October, pp. 3470-3472.

Chau, K.T., Sun, Q., Fan, Y. and Cheng, M. (2005) 'Torque ripple minimization of doubly salient permanent magnet motors.' *IEEE Transactions on Energy Conversion*, Vol. 20, No. 2, June, pp. 352-358.

Chau, K.T., Wong, Y.S. and Chan, C.C. (1999) 'An overview of energy sources for electric vehicles', *Energy Conversion and Management*, Vol. 40, No. 10, July, pp. 1021-1039.

Chau, K.T., Zhang, D., Jiang, J.Z., Liu, C. and Zhang, Y. (2007) 'Design of a magnetic-geared outer-rotor permanent-magnet brushless motor for electric vehicles,' *IEEE Transactions on Magnetics*, Vol. 43, No. 6, June, pp. 2504-2506.

Cheng, M., Chau, K.T. and Chan, C.C. (2001) 'Design and analysis of a new doubly salient permanent magnet motor', *IEEE Transactions on Magnetics*, Vol. 37, No. 4, July, pp. 3012-3020.

Cheng, M., Chau, K.T. and Chan, C.C. (2003) 'New split-winding doubly salient permanent magnet motor drive', *IEEE Transactions on Aerospace and Electronic Systems*, Vol. 39, No. 1, January, pp. 202-210.

Deodhar, R.P., Andersson, S., Boldea, I. and Miller, T.J.E. (1997) 'The flux-reversal machine: a new brushless doubly-salient permanent magnet machine', *IEEE Transactions on Industry Applications*, Vol. 33, No. 4, July/August, pp. 925-934.

Dubey, G. (1989) *Power Semiconductor Controlled Drives*. Prentice Hall.

Ehsani, M., Gao, Y., Gay, S.E. and Emadi, A. (2005) *Modern Electric, Hybrid Electric, and Fuel Cell Vehicles: Fundamentals, Theory, and Design*. Boca Raton: CRC Press.

Ehsani, M., Rahman, K.M. and Toliyat, H.A. (1997) 'Propulsion system design of electric and hybrid vehicles', *IEEE Transactions on Industrial Electronics*, Vol. 44, No. 1, February, pp. 19-27.

Gan, J., Chau, K.T., Chan, C.C. and Jiang, J.Z. (2000) 'A new surface-inset, permanent-magnet, brushless DC motor drive for electric vehicles', *IEEE Transactions on Magnetics*, Vol. 36, No. 5, September, pp. 3810-3818.

Gong, Y., Chau, K.T., Jiang, J.Z., Yu, C. and Li, W. (2009a) 'Analysis of doubly salient memory motors using Preisach theory', *IEEE Transactions on Magnetics*, Vol. 45, No. 10, October, pp. 4676-4679.

Gong, Y., Chau, K.T., Jiang, J.Z., Yu, C. and Li, W. (2009b) 'Design of doubly salient permanent magnet motors with minimum torque ripple', *IEEE Transactions on Magnetics,* Vol. 45, No. 10, October, pp. 4704-4707.

Harris, M.R. (1997) 'Comparison of alternative topologies for VRPM (transverse-flux) electrical machines', *Proc. IEE Colloquium on New Topologies for Permanent Magnet Machines*, London, June, pp. 2/1-2/7.

Inderka, R.B., Menne, M. and De Doncker, R.W.A.A. (2002) 'Control of switched reluctance drives for electric vehicle applications', *IEEE Transactions on Industrial Electronics*, Vol. 49, No. 1, February, pp. 48-53.

Jian, L. and Chau, K.T. (2010a) 'A coaxial magnetic gear with Halbach permanent magnet arrays', *IEEE Transactions on Energy Conversion*,

Vol. 25, No. 2, June, pp. 319-328.
Jian, L. and Chau, K.T. (2010b) 'Design and analysis of a magnetic-geared electronic-continuously variable transmission system using finite element method', *Progress In Electromagnetics Research*, Vol. 107, pp. 47-61.
Jian, L., Chau, K.T., Gong, Y., Jiang, J.Z., Yu, C. and Li, W. (2009) 'Comparison of coaxial magnetic gears with different topologies', *IEEE Transactions on Magnetics*, Vol. 45, No. 10, October, pp. 4526-4529.
Kamiya, M. (2006) 'Development of traction drive motors for the Toyota hybrid system', *IEEJ Transactions on Industry Applications*, Vol. 126, No. 4, July, pp. 473-479.
Kim, Y., Kook, Y. and Ko, Y. (1997) 'A new technique of reducing torque ripples for BDCM drives', *IEEE Transactions on Industrial Electronics*, Vol. 44, No. 5, October, 735-739.
Li, J., Chau, K.T., Jiang, J.Z., Liu, C. and Li, W. (2010) 'A new efficient permanent-magnet vernier machine for wind power generation', *IEEE Transactions on Magnetics*, Vol. 45, No. 6, June, pp. 1475-1478
Li, W. and Chau, K.T. (2010) 'Design and analysis of a novel linear transverse flux permanent magnet motor using HTS magnetic shielding', *IEEE Transactions on Applied Superconductivity*, Vol. 20, No. 3, June, pp. 1106-1109.
Liao, Y., Liang, F. and Lipo, T. A. (1995) 'A novel permanent magnet motor with doubly salient structure', *IEEE Transactions on Industry Applications*, Vol. 31, No. 5, September/October, pp. 1069-1078.
Liu, C., Chau, K.T. and Jiang, J.Z. (2010) 'A permanent-magnet hybrid brushless integrated-starter-generator for hybrid electric vehicles', *IEEE Transactions on Industrial Electronics*, Vol. 57, No. 12, December, pp. 4055-4064.
Liu, C., Chau, K.T., Li, W. and Yu, C. (2009a) 'Efficiency optimization of a permanent-magnet hybrid brushless machine using DC field current control', *IEEE Transactions on Magnetics*, Vol. 45, No. 10, October, pp. 4652-4655.
Liu, C., Chau, K.T., Jiang, J.Z. and Niu, S. (2008) 'Comparison of stator-permanent-magnet brushless machines', *IEEE Transactions on Magnetics*, Vol. 44, No. 11, November, pp. 4405-4408.
Liu, X., Chau, K.T., Jiang, J.Z. and Yu, C. (2009b) 'Design and analysis of interior-magnet outer-rotor concentric magnetic gears', *Journal of Applied Physics*, Vol. 105, No. 7, April, Paper No. 07F101, pp. 1-3.
Long, S.A., Zhu, Z.Q. and Howe, D. (2005) 'Effectiveness of active noise and vibration cancellation for switched reluctance machines operating under alternative control strategies', *IEEE Transactions on Energy*

Conversion, Vol. 20, No. 4, December, pp. 792-801.
Miller, J.M. (2006) 'Hybrid electric vehicle propulsion system architectures of the e-CVT type', *IEEE Transactions on Power Electronics*, Vol. 21, No. 3, May, pp. 756-767.
Miller, T.J.E. (1993) *Switched Reluctance Motors and Their Control*, Oxford University Press.
Mueller, M.A. and Baker, N.J. (2003) 'Modelling the performance of the vernier hybrid machine', *IEE Proceedings - Electric Power Applications*, Vol. 150, No. 6, November, pp. 647-654.
Novotny, D.W. and Lipo, T.A. (1996) *Vector Control and Dynamics of AC Drives*. Oxford University Press.
Ostovic, V. (2003) 'Memory motor', *IEEE Industry Applications Magazine*, Vol. 9, No. 1, January/February, pp. 52-61.
Pillay, P. and Krishnan, R. (1988) 'Modeling of permanent magnet motor drives.' *IEEE Transactions on Industrial Electronics*, Vol. 35, No. 4, November. pp. 537-541.
Rahman, K.M., Fahimi, B., Suresh, G., Rajarathnam, A.V. and Ehsani, M. (2000) 'Advantages of switched reluctance motor applications to EV and HEV: design and control issues', *IEEE Transactions on Industry Applications*, Vol. 36, No. 1, January/February, pp. 111-121.
Safi, S.K., Acarnley, P.P. and Jack, A.G. (1995) 'Analysis and simulation of the high-speed torque performance of brushless DC motor drives', *IEE Proceedings - Electric Power Applications*, Vol. 142, No. 3, May, pp. 191-200.
Soong, W.L. and Ertugrul, N. (2002) 'Field-weakening performance of interior permanent-magnet motors', *IEEE Transactions on Industry Applications*, Vol. 38, No. 5, September/October, pp. 1251-1258.
Spooner, E. and Haydock, L. (2003). Vernier hybrid machines. *IEE Proceedings - Electric Power Applications*, Vol. 150, No. 6, November, pp. 655-662.
Toba, A. and Lipo, T.A. (1999) 'Novel dual-excitation permanent magnet vernier machine', *Proc. IEEE Conference on Industry Applications*, Phoenix, October, pp. 2539-2544.
Wang, J., Chau, K.T., Jiang, J.Z. and Yu, C. (2008) 'Design and analysis of a transverse flux permanent-magnet machine using three-dimensional scalar magnetic potential finite element method', *Journal of Applied Physics*, Vol. 103, No. 7, April, Paper No. 7F107, pp. 1-3.
Wang, Y., Chau, K.T., Chan, C.C. and Jiang, J.Z. (2002) 'Design and analysis of a new multiphase polygonal-winding permanent-magnet brushless DC machine', *IEEE Transactions on Magnetics*, Vol. 38, No. 5, September, pp. 3258-3260.

Weh, H., Hoffman, H. and Landrath, J. (1988) 'New permanent magnet excited synchronous machine with high efficiency at low speeds', *Proc. International Conference on Electrical Machines*, Pisa, September, pp. 35-40.

Yu, C., Chau, K.T., Liu, X. and Jiang, J.Z. (2008). A flux-mnemonic permanent magnet brushless motor for electric vehicles. *Journal of Applied Physics*, Vol. 103, No. 7, April, Paper No. 07F103, pp. 1-3.

Zhu, X., Chau, K.T., Cheng, M. and Yu, C. (2008) 'Design and control of a flux-controllable stator-permanent magnet brushless motor drive', *Journal of Applied Physics*, Vol. 103, No. 7, April, Paper No. 7F134, pp. 1-3.

Zhu, X., Cheng, M., Chau, K.T. and Yu, C. (2009) 'Torque ripple minimization of flux-controllable stator-permanent-magnet brushless motors using harmonic current injection', *Journal of Applied Physics*, Vol. 105, No. 7, April, Paper No. 07F102, pp. 1-3.

Zhu, Z.Q. and Howe, D. (2007). Electrical machines and drives for electric, hybrid and fuel cell vehicles. *IEEE Proceedings*, Vol. 95, No. 4, April, pp. 746-765.

Zhu, Z.Q., Chen Y.S. and Howe, D. (2000) 'On-line optimal field weakening control of permanent magnet brushless AC drives', *IEEE Transactions on Industry Applications*, Vol. 36, No. 6, November/December, pp. 1661-1668.

Zhu, Z.Q., Pang, Y., Howe, D., Iwasaki, S., Deodhar, R. and Pride, A. (2005) 'Analysis of electromagnetic performance of flux-switching permanent magnet machines by non-linear adaptive lumped parameter magnetic circuit model', *IEEE Transactions on Magnetics*, Vol. 41, No. 11, November, pp. 4277-4287.

Figure 1 Classification of vehicles

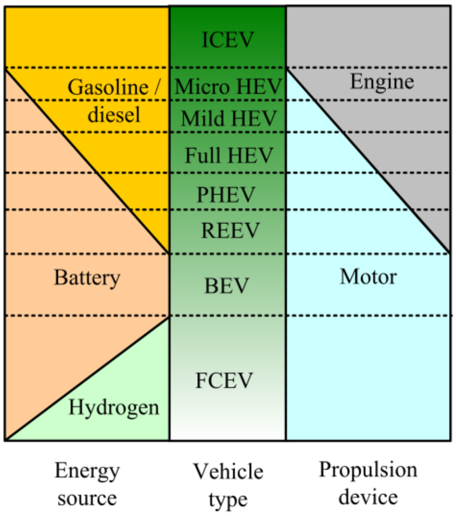

Figure 2 Existing machine topologies for EVs and HEVs

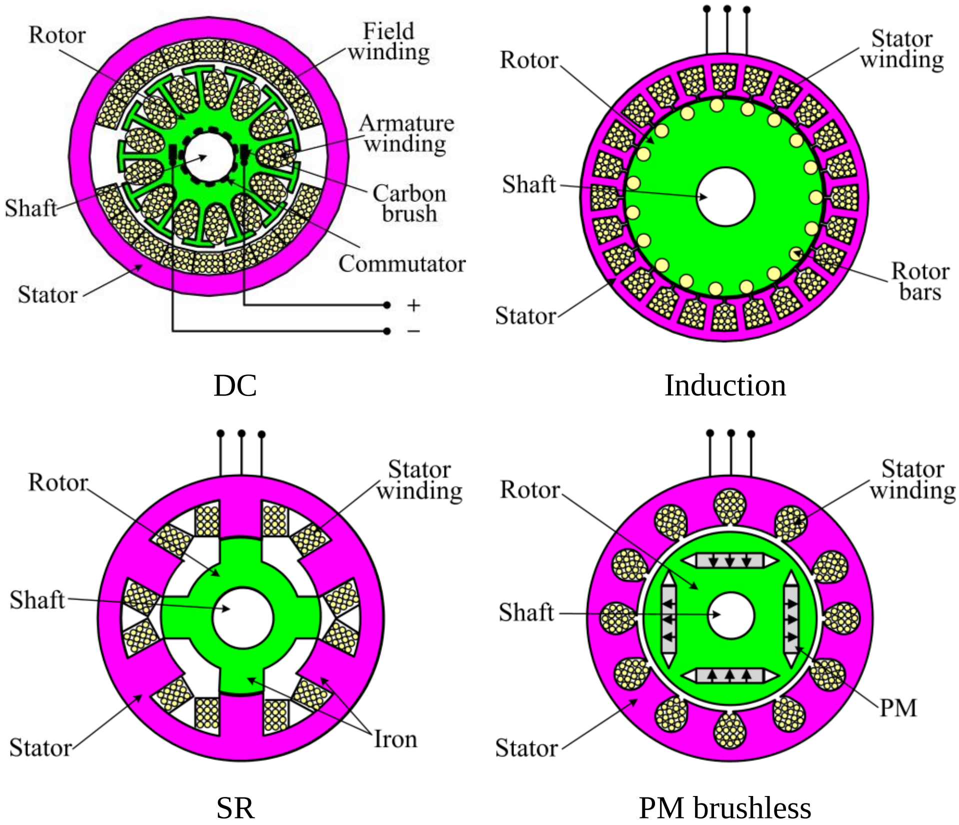

Figure 3 DC machine types

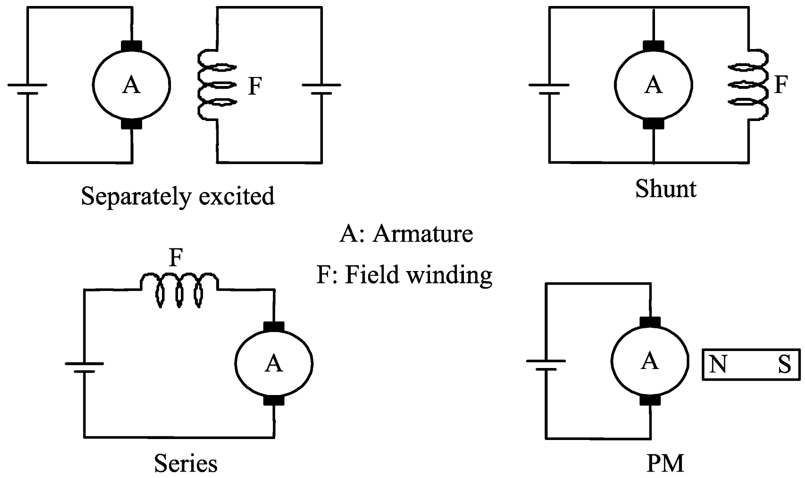

Figure 4 Induction machine operations

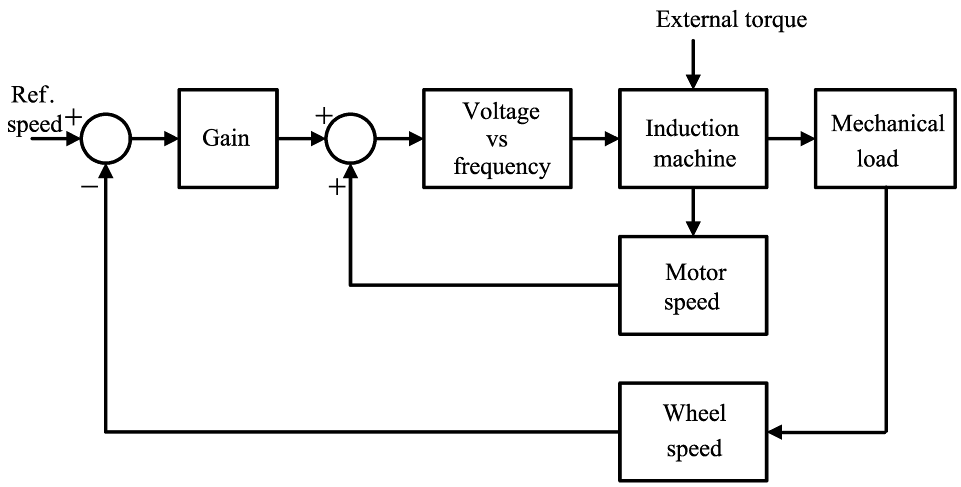

VVVF control

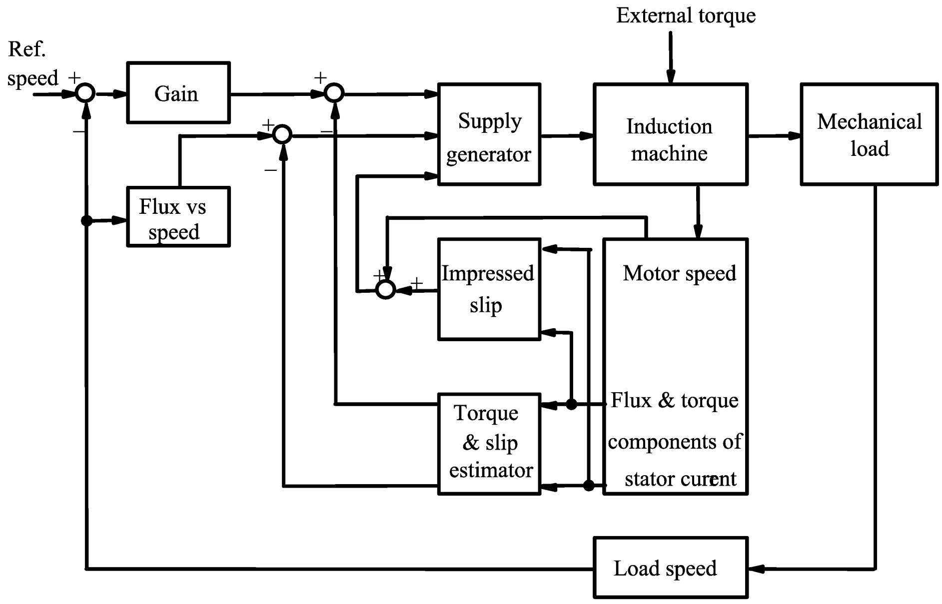
External torque
Ref.
speed
Gain
Supply
generator
Induction
machine
Mechanical
load
Flux vs
speed
Impressed
slip
Motor speed
Flux & torque
components of
stator current
Torque
& slip
estimator
Load speed

FOC

Figure 5 SR machine operations

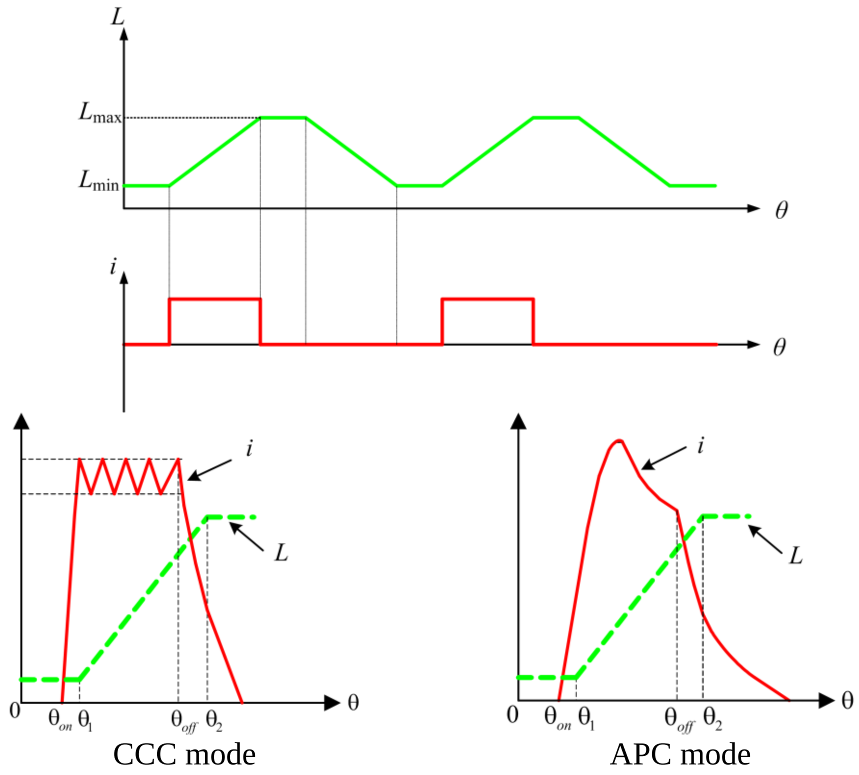

Figure 6 PM brushless machine types

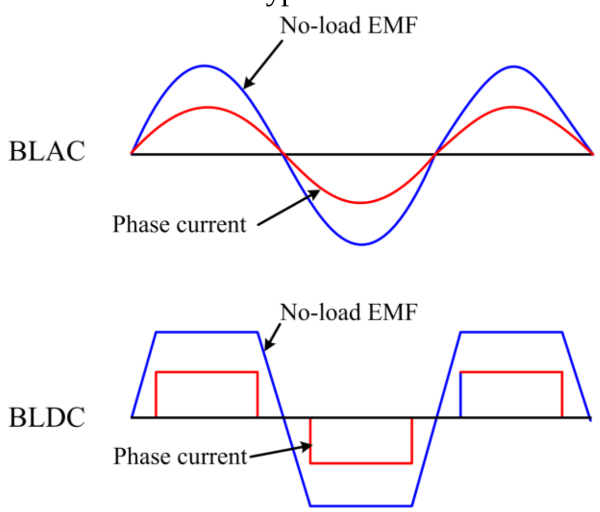

Figure 7 PM brushless machine topologies

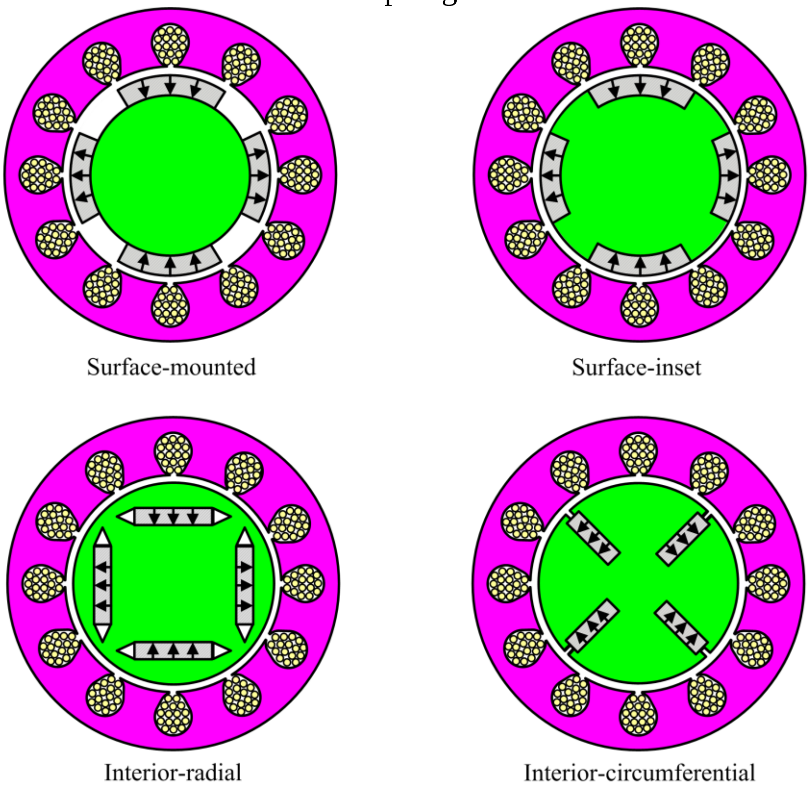

Figure 8 Classification of electric machines for EVs and HEVs

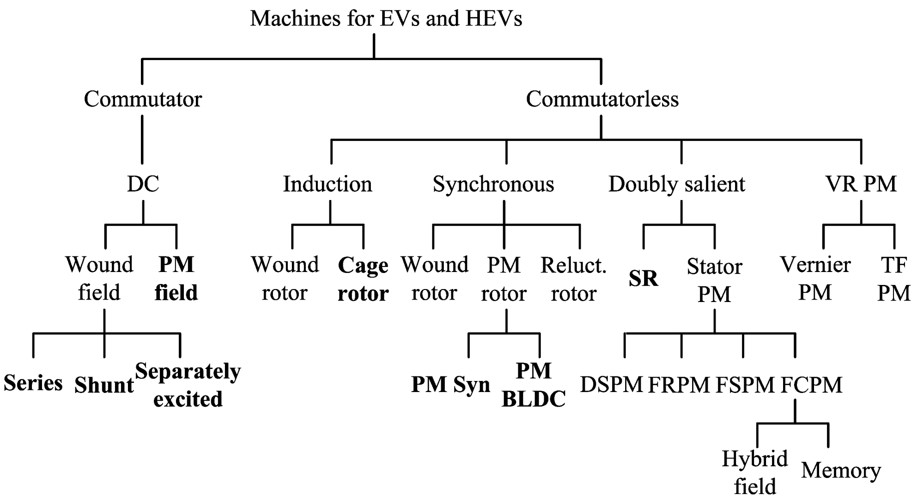

Figure 9 Stator-PM machine topologies

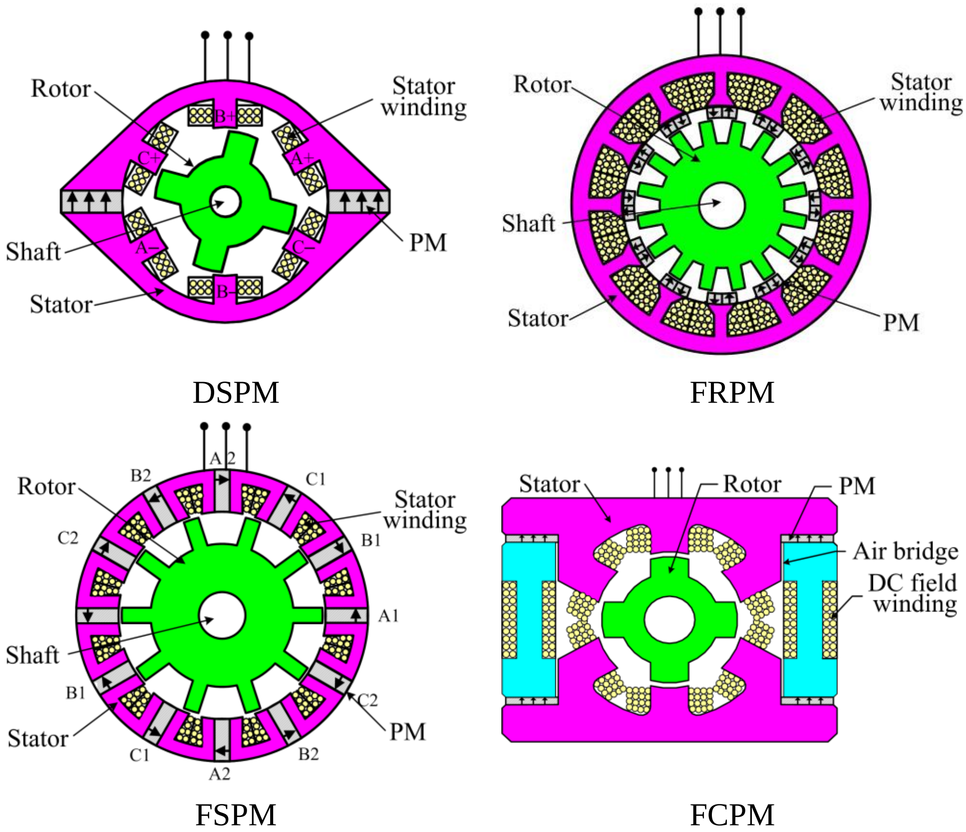

Figure 10 DSPM machine operation

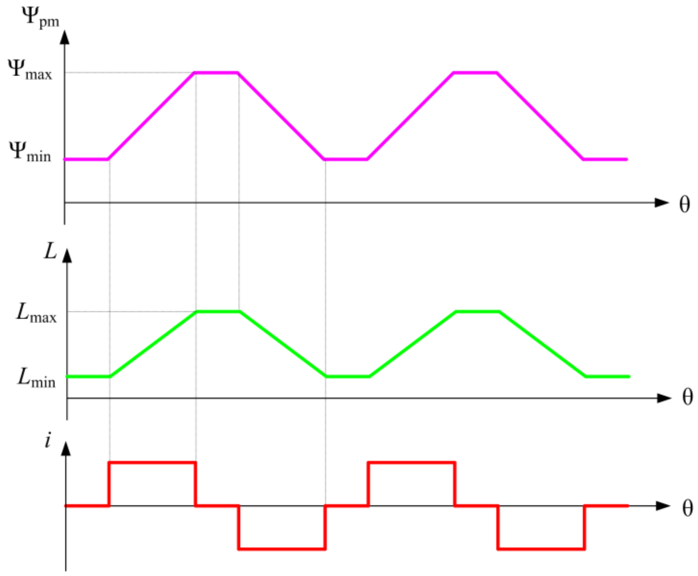

Figure 11 Performances of hybrid-field DSPM machine with and without flux control

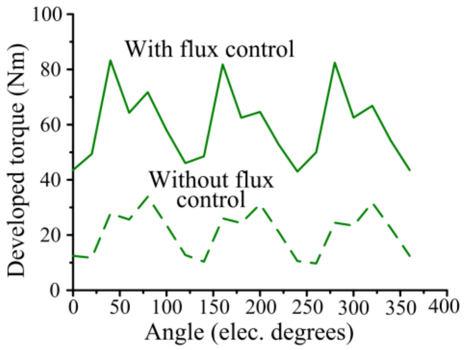

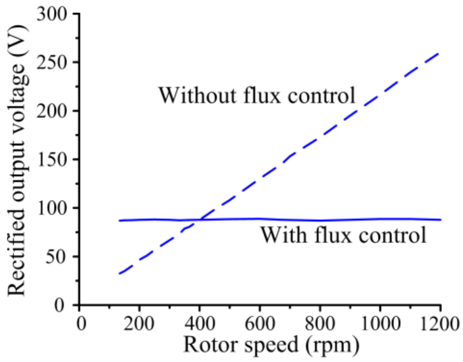

Figure 12 Outer-rotor memory DSPM machine topology and operation

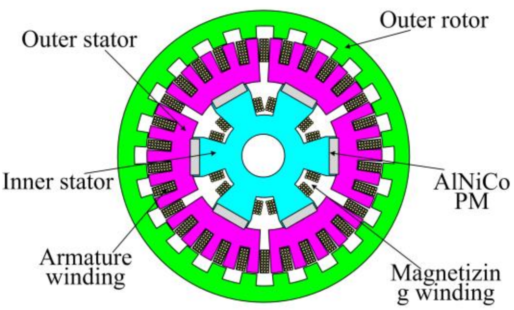

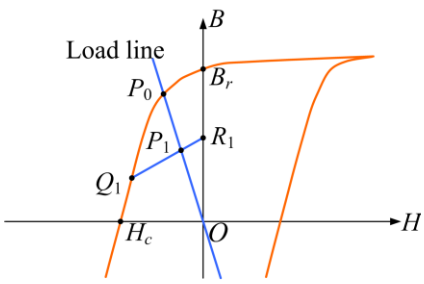

AlNiCo PM demagnetization curve

Figure 13 VR PM machine topologies

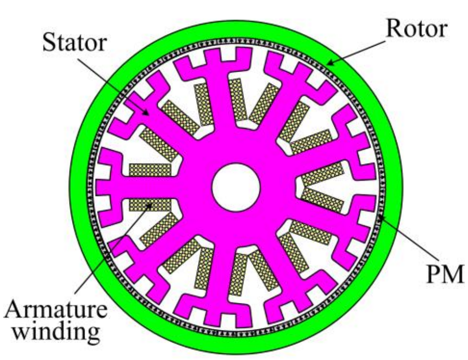

VPM

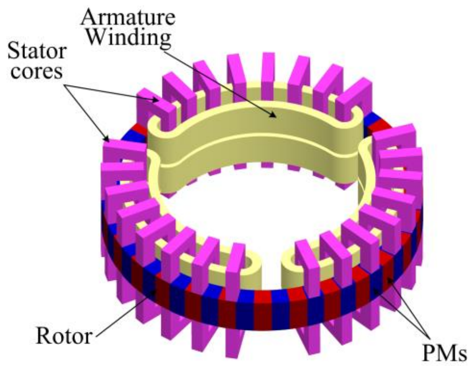

TFPM

Figure 14 Comparison of in-wheel PM brushless machines

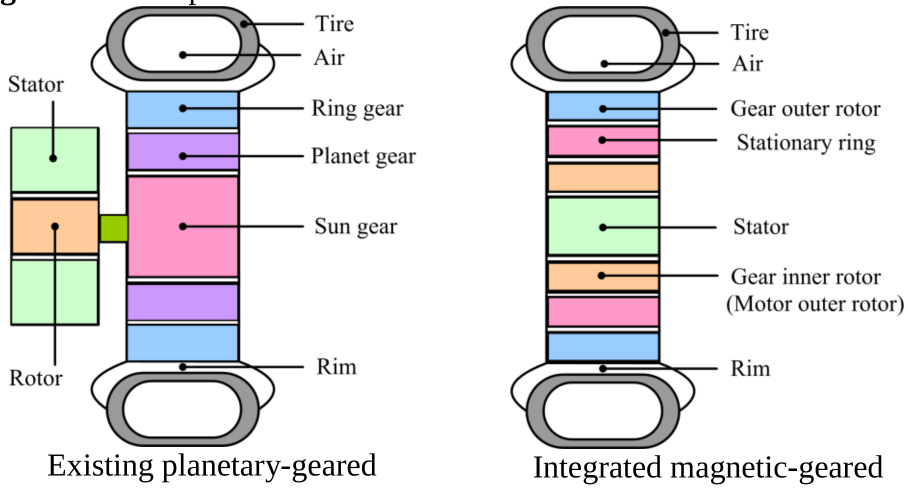

Figure 15 Integrated magnetic-geared PM brushless machine topology and operation

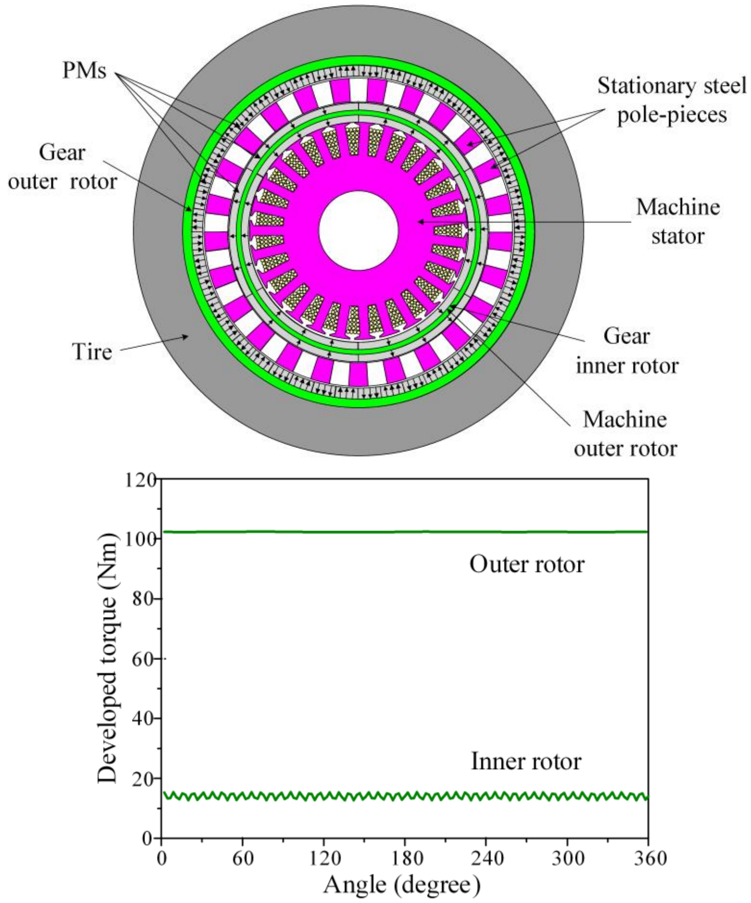

Figure 16 Comparison of EVT PM machine systems